

## Article

# Two-Step Macromolecule Separation Process with Acid Pretreatment and High-Shear-Assisted Extraction for Microalgae-Based Biorefinery

Donghyun Kim <sup>1</sup>, Seul-Gi Kang <sup>2</sup>, Yong Keun Chang <sup>2</sup> and Minsoo Kwak <sup>2,\*</sup>

<sup>1</sup> Department of Chemical Engineering, College of Engineering, Qatar University, Doha P.O. Box 2713, Qatar; dkim@qu.edu.qa

<sup>2</sup> Department of Chemical and Biomolecular Engineering, KAIST, 291 Daehak-ro, Yuseong-gu, Daejeon 34141, Republic of Korea; ychang@kaist.ac.kr (Y.K.C.)

\* Correspondence: minsoo.kwak@kaist.ac.kr

**Abstract:** A simple two-stage extraction and recovery method for macromolecules from microalgae biomass, termed CASS (concentrating the microalgae solution, acid pretreatment, high-shear-assisted lipid extraction, and separation), was developed. This method effectively processed the wet biomass of *Chlorella* sp. ABC-001 at a moderately low biomass concentration (50 g/L). The optimal conditions were acid pretreatment with 5 wt.% H<sub>2</sub>SO<sub>4</sub> at 100 °C for 1 h, followed by high-shear extraction using hexane at 3000 rpm for 30 min. The acid pretreatment hydrolyzed carbohydrates and phospholipids, disrupting the cell wall and membrane, while high-shear mixing enhanced mass transfer rates between solvents and lipids, overcoming the hydraulic barrier at the cell surface. Within 10 min after completing the process, the extraction mixture achieved natural phase separation into water, solvent, and biomass residue layers, each enriched with carbohydrates, lipids, and proteins, respectively. The CASS process demonstrated high esterifiable lipid yields (91%), along with substantial recovery of glucose (90%) and proteins (100%). The stable phase separation prevented emulsion formation, simplifying downstream processing. This study presents the results on cell disruption, optimal acid treatment concentration, and high-shear mixing to achieve macromolecule separation, expanding the lipid-centric microalgal process to a comprehensive biorefinery concept.

**Keywords:** microalgae; biorefinery; macromolecule; acid pretreatment; high-shear mixer



**Citation:** Kim, D.; Kang, S.-G.; Chang, Y.K.; Kwak, M. Two-Step Macromolecule Separation Process with Acid Pretreatment and High-Shear-Assisted Extraction for Microalgae-Based Biorefinery. *Sustainability* **2024**, *16*, 7589. <https://doi.org/10.3390/su16177589>

Academic Editors: Domenico Licursi and Juan Hernández Adrover

Received: 3 August 2024

Revised: 27 August 2024

Accepted: 28 August 2024

Published: 2 September 2024



**Copyright:** © 2024 by the authors. Licensee MDPI, Basel, Switzerland. This article is an open access article distributed under the terms and conditions of the Creative Commons Attribution (CC BY) license (<https://creativecommons.org/licenses/by/4.0/>).

## 1. Introduction

Recent trends in Renewable Fuel Standards (RFS) indicate a growing emphasis on increasing the use of renewable fuels in the transportation sector [1]. The RFS determines a minimum volume of renewable fuel to be blended into U.S. transportation fuel each year, with specific classifications for different types of biofuels like conventional biofuel, advanced biofuel, cellulosic biofuel, and biomass-based diesel [2]. In addition, ASTM D7566 recently approved blends of up to 10% converted triglyceride oil derived from microalgae for Sustainable Aviation Fuel (SAF) [3]. Microalgae have been studied as a third-generation biofuel feedstock, offering advantages such as higher growth rates, biomass yield, and oil productivity on an areal basis compared to other counterparts [4–6]. Nonetheless, the higher production costs than conventional fossil fuels have hindered its commercial viability. To establish a more sustainable production model, it is crucial to utilize non-lipid macromolecules such as carbohydrates and proteins [7]. This approach expands the scope of microalgae-based processes from a sole focus on lipid-centric biofuel production to encompass comprehensive biorefinery concepts [8].

A complete utilization of biomass macromolecules faces numerous challenges due to the complex biochemical composition of microalgae [9]. Carbohydrates and proteins, potential carbon and nitrogen sources for the subsequent cultivation of microbes, are

accumulated during the late exponential phase of microalgae growth [10]. Due to their hydrophilicity, carbohydrates and proteins may remain in the biomass residue and water phase, leading to potential issues during lipid extraction [11]. Those macromolecules, especially proteins, can cause the emulsification of organic and water phases with the biomass residue, resulting in a significant loss in lipid yield and additional downstream processing costs [12]. On the other hand, phospholipids, another type of well-known bio-surfactant, not only cause emulsification but also act as poison for catalysts in the lipid conversion process, e.g., hydrotreating or hydrocracking reactions [13]. Other inorganic compounds such as  $\text{Ca}^{2+}$ ,  $\text{Mg}^{2+}$ , and  $\text{K}^+$ , which are remaining nutrients, also exist in extracted lipids and induce catalytic poisoning [14]. To increase the lipid extraction efficiency and economic feasibility of microalgal biorefinery, it is necessary to efficiently separate macromolecules and inorganic compounds from extracted crude lipids.

Thermochemical routes for the cell disruption process have been widely studied to increase lipid extraction yield from wet biomass [15]. Acid pretreatment under high temperatures induces an acidic hydrolysis reaction of various cellular molecules, including the cellulosic cell wall, carbohydrates, proteins, and polar lipids, e.g., phospholipids and glucolipids [16–18]. This method has been employed for a relatively low concentration biomass (<60 g/L) [19–26] because highly concentrated biomass requires much higher acidic conditions, which may reduce process operability by corrosion [27]. However, after acid pretreatment at low biomass concentrations, the lipid recovery process with non-polar solvents like hexane may take a long time. This is because the water contents in the biomass form a hydrophilic barrier, preventing hexane from reaching the lipid droplets and requiring extended process times to capture the lipids [4]. In the previous reports, our group developed an energy-efficient lipid extraction process using a high-shear mixer from wet algal biomass [12]. The high-shear mixer (HSM), which is a unique mixing equipment that consists of a rotor–stator assembly, is capable of producing high rotor tip speed (ranging from 10 to 50 m/s), high shear rates (ranging from 20,000 to 100,000  $\text{s}^{-1}$ ), and highly localized energy dissipation rates near the mixing head [28]. HSM has been proven to minimize the water barriers and dramatically increase mass transfer rate through strong turbulent mixing. However, the authors focused on lipid extraction from the concentrated biomass (>250 g/L) without utilizing other biomass components, which requires more studies about major nutrients (carbohydrates and protein) recovery and impurity removals to develop final concepts of bio-algal refineries [12]. Furthermore, highly concentrated biomass is difficult to achieve due to the energy-intensive harvesting technology, which increases the cost of the overall process.

Herein, we have developed a process that combines thermochemical treatment and high-shear mixing for the fractionation of macromolecules and impurities, aiming for a complete utilization of biomass. *Chlorella* sp. ABC-001, which has a unique characteristic of accumulating both carbohydrates and lipids during the stationary growth phase under nitrogen-depleted conditions, was used as a model biomass [29]. The CASS process proposed in this paper comprises four stages: (1) concentrating the microalgae solution, (2) acid pretreatment, (3) high-shear-assisted lipid extraction, and (4) separation (Figure 1). The application of high shear during lipid extraction makes the process operable at a moderate biomass concentration (50 g/L), which can be achieved by energy-efficient membrane harvesting technology [30,31]. This approach hypothesizes as follows: (1) Hydrolysis breaks down the carbohydrate contents of the microalgae, e.g., cellulosic cell wall and starch, into smaller sugars, e.g., monosaccharides, in the aqueous phase. (2) The acids detach the hydrophilic heads from the phospholipids, leaving behind nonpolar hydrocarbon tails, which are then separated into the aqueous phase. (3) Both high lipid extraction and glucose recovery yield are achieved by high-shear mixing, which enhances the mass transfer rate between the water/nonpolar solvent and biomass, overcoming the hydraulic barrier at the surface of the cells when the solvents contact the concentrated wet biomass. This study evaluates the cell disruption, separation of macromolecules, and their compositions observed in each stage, suggesting a sustainable biorefinery concept based on the CASS process.

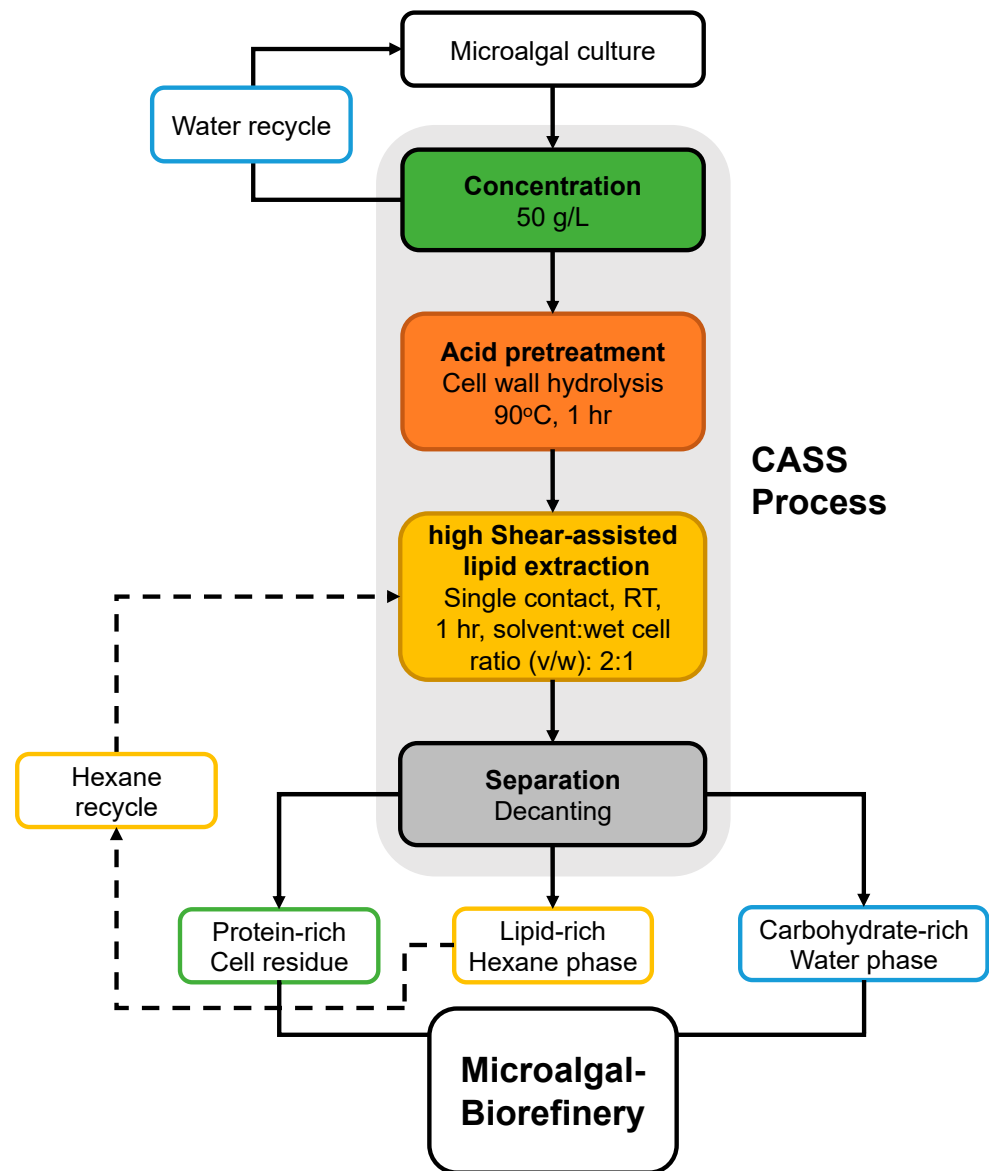


**Figure 1.** Microalgal-based biorefinery based on the CASS process.

## 2. Materials and Methods

### 2.1. Materials

*Chlorella* sp. ABC-001 was selected as the model strain due to its high content of lipids and total carbohydrates compared to other microalgae strains [29]. The microalgae was cultivated in an indoor photobioreactor (PBR) system by KIER (Korea Institute of Energy Research). The biomass was harvested and dewatered by centrifuge and freeze-dryer, respectively, and stored in a refrigerator (4 °C) until use. Bulk N-hexane (>95%) for lipid extraction was purchased from Samchun Chemical (Pyeongtaek, Republic of Korea). Chloroform, methanol (HPLC grade), sulfuric acid (99.8%), FAME mix, and heptadecanoic acid ( $\geq 99.5\%$ ) were purchased from Merck (Darmstadt, Germany). Nitrogen (N<sub>2</sub>) for hexane evaporation and pure compressed air, helium (He), and hydrogen (H<sub>2</sub>) gases for gas chromatography (GC) were purchased from Samo Gas (Daejeon, Republic of Korea).

### 2.2. Biochemical Composition Analysis

The composition of *Chlorella* sp. ABC-001 was analyzed prior to the extraction experiment. The total amount of lipids was quantified by the modified Folch method in gravimetric yield [32]. A total of 50 mg of fully dried cells and 10 mL of chloroform/methanol

(2:1 *v/v*) solution were treated in a sonication bath for 1 h at maximum amplitude. After pretreatment, the solution was mixed with 5 mL of water for phase separation and separated by centrifuge. Then, 3 mL of chloroform was decanted into the pre-weighed aluminum dish and evaporated under a fume hood. Residues were weighed to calculate the total lipid contents by the following equation.

$$\text{Total lipid content (wt.\%)} = (W_l - W_d) \times \frac{V_t}{V_d \times W_b} \quad (1)$$

$W_l$ ,  $W_d$ , and  $W_b$  represent the weight of the aluminum dish with lipids, aluminum dish, and biomass, respectively.  $V_t$  and  $V_d$  represent the total volume and decanted volume of chloroform, respectively.

The total esterifiable lipids were analyzed by an in situ transesterification method [33]. A total of 20 mg of dry biomass was mixed with chloroform/methanol (2:1 *v/v*) and vortexed for 5 min with an additional 1 mL of methanol, internal standard (C17:0, 0.5 mg), and 0.3 mL of sulfuric acid. The mixture was heated at 100 °C for 20 min to convert lipids into fatty acid methyl ester (FAME). After phase separation by adding distilled water, the organic phase containing FAME was filtrated with a 0.22 µm polytetrafluoroethylene (PTFE) filter. The filtrate was analyzed to characterize FAME content by gas chromatography 6890 (Agilent Technologies, Santa Clara, CA, USA) with a flame-ionized detector (GC-FID) and an INNOWAX capillary column (30 m × 0.32 mm × 0.5 µm, Agilent, USA).

Total carbohydrate content was analyzed by colorimetric method using phenol-sulfuric acid, using glucose as a standard [34]. A total of 1 mL of algal suspension solution (0.5 g/L) was mixed with 1 mL of phenol (5% *w/v*) and sulfuric acid (95%, 5 mL) and cooled in a dark room for 30 min. The total carbohydrate content was determined by UV absorbance at 470 nm. The calibration curve was obtained using a glucose standard. The monosaccharide content was analyzed using high-performance liquid chromatography [35]. A total of 0.6 g of dry biomass was mixed with 60 mL of 2 N nitric acid. The mixture was then heated at 90 °C for 3 h and 1 mL was sampled every 30 min. Each sample was filtered and soluble carbohydrates (glucose, fucose, xylose, galactose, mannose, rhamnose) were analyzed by high-performance liquid chromatography with refractive index detection (HPLC-RID) with HPX-87H column, while 0.05 mM sulfuric acid was used as the mobile phase. The monosaccharide recovery was estimated as follows:

$$\text{Monosaccharide recovery (\%)} = \frac{\text{Hydrolyzed soluble carbohydrate content}}{\text{Total soluble carbohydrate content}} \times 100 \quad (2)$$

where total soluble carbohydrate content represents the content of monosaccharide in dry biomass hydrolyzed by the method described.

Ash content was measured gravimetrically after calcination. Before calcination, an aluminum dish was preheated at 550 °C for 4 h. A total of 0.5 g of dried biomass was heated with the pretreated aluminum dish in a furnace at 575 °C for 4 h, and the residue was measured by a gravimetrical-like total lipid analysis method [36]. The protein content was calculated by subtracting all the other components (total lipids, carbohydrates, ash) from 100%. All experiments for the biochemical composition analysis were carried out in triplicate.

### 2.3. Acid Pretreatment of Wet Biomass

Acid pretreatment of concentrated wet biomass (50 g/L) was carried out to produce hydrolyzed wet biomass. Firstly, 0.5 g of dried biomass was dispersed in 10 mL of distilled water in a 50 mL Duran bottle to prepare the model concentrated wet biomass. Sulfuric acid (99.8%) was then added to the wet biomass at specific concentrations, and mixing was performed with a magnetic stirrer by using a conventional heating plate. After mixing, the sample was cooled to room temperature before adding 15 mL n-hexane. The mixture was stirred again at 1000 rpm at room temperature for 12 h to fully extract lipids from the

microalgal cells. The organic solvent layer (n-hexane containing lipids) and aqueous phase (containing cell debris) were separated by centrifugation at 4000 rpm for 10 min. A known volume of lipid-containing solvent was transferred to a pre-weighed aluminum dish and evaporated in a fume hood. The extracted lipid content was analyzed by a gravimetric method, and lipid recovery was calculated using the following equation.

$$\text{Lipid recovery yield (\%)} = \frac{\text{Extracted lipid content}}{\text{Total lipid content}} \times 100 \quad (3)$$

The effects of acid concentration, acid treatment time, and temperature on lipid recovery were investigated. Acid concentrations were varied from 0.5 to 5 vol.% (0.5, 1, 3, 5), equivalent to 0.18, 0.36, 1.08 and 1.8 N, respectively, at 100 °C for 1 h. The acid treatment time was varied from 5, 10, 30, and 60 min under a static condition of 5 vol.% of sulfuric acid at 100 °C. The temperature of acid treatment was varied from 70, 80, 90, 100, and 120 °C under a static condition of 5 vol.% of sulfuric acid and 60 min of treatment time. To verify the effects of treatment temperature on cell morphology, microscopic images of disrupted cells were obtained with a DM2500 microscope equipped with a DFC425C camera (Leica Microsystems, Wetzlar, Germany). All experiments were carried out in duplicates.

#### 2.4. High Shear-Assisted Lipid Extraction

Following the acid pretreatment of wet biomass, a lipid extraction process using a high-shear mixer (HSM) was developed to enhance the lipid extraction yield and reduce the extraction time. A conventional lab-scale HSM, L5M-A (Silverson, Chesham, UK), was used in this research. The diameter of the rotor and the rotor–stator gap distance were 15.7 and 0.075 mm, respectively. A commercial vertical screen equipped with the L5M-A, which had 12 slits, each measuring 2 × 10 mm, was used. The surface of the HSM was coated with ethylene tetrafluoroethylene (ETFE) EC-6515 (Dalkin, Osaka, Japan) to reduce the attachment of biomass.

The extraction efficiency of the conventional stirrer and HSM was compared with varying rotational speed and treatment time. The conventional stirrer was operated at 500, 750, and 1000 rpm for 0, 1.5, 3, 6, 9, and 12 h. The HSM was operated at 1000, 2000, and 3000 rpm for 0, 5, 10, 30, 60, and 90 min. At each time point, a known volume of lipid-containing hexane was sampled and decanted into a 15 mL vertical glass tube. The solvent was then evaporated using a nitrogen purge, and the lipids remaining in the tube were converted into FAME by the in situ transesterification method and analyzed by GC (using the same methods as previously mentioned in Section 2.2). Esterifiable lipid yield was calculated using the following equation.

$$\text{Esterifiable lipid yield (\%)} = \frac{\text{Extracted esterifiable lipids}}{\text{Total esterifiable lipids}} \times 100 \quad (4)$$

#### 2.5. Characterization of Oil, Water, and Solid Phase Products

Detailed characterization of biomass, oil phase, and water phase was performed to find a distribution of macromolecules. For the oil phase and water phase, lipid and carbohydrate characterization were performed, respectively. The solid phase, lipid-extracted algae (LEA), was separated and analyzed for lipid content and esterifiable content by the method described in Section 2.2. The ash content of oil, water, and solid phase was analyzed by the method described in Section 2.2. The carbohydrate and protein content of the solid phase was calculated by subtracting extracted macromolecule contents in the oil and water phase, respectively. Elemental analysis (C, H, O, N, S) was performed on raw biomass, extracted oil, and LEA using an elemental analyzer, FLASH 2000 series (Thermo Scientific, Waltham, MA, USA).

Inorganic element analysis (P, Ca, Na, K, Cu, Zn, Mg) of oil, water, and solid phase was performed using inductively coupled plasma–optical emission spectroscopy (ICP-OES). For oil and water phase analysis, the solvent and water were fully evaporated using a vacuum



evaporator. Pre-weighed samples were pretreated with nitric acid to remove any organic content. A 40 mg oil sample was diluted with V-SOLV™ (VHG Labs, Manchester, UK) solution and CONOSTAN Multi-Element Standard (150-021-015) was used as the standard. ICP-OES analysis conditions for quantifying metal and phosphorus contents are described as follows: plasma power 1400 W, pump speed 15 rpm, coolant flow 12 L/min, auxiliary flow 1.5 L/min, nebulizer flow 0.6 L/min, oxygen flow 0.2 L/min. The initial content was determined by analyzing the crude oil extracted by the modified Folch method described in Section 2.2.

### 3. Results and Discussion

#### 3.1. Biochemical Composition of *Chlorella* sp. ABC-001

Table 1 shows the biochemical composition of *Chlorella* sp. ABC-001 used for the CASS process. The lipid content of the biomass was 35.7 wt.%, which contained 29.8 wt.% of esterifiable lipids and 4.9 wt.% of non-esterifiable lipids (e.g., chlorophyll, hydrocarbon). The carbohydrate content of the biomass, which is another major nutrient of ABC-001, was 40.1 wt.%, which contained 19.1 wt.% of glucose that could be converted into valuable biochemicals, e.g., bioethanol and biopolymer, through fermentation [37]. The rest of the biomass consisted of 18.6 wt.% of proteins and 5.5 wt.% of ashes. These high esterifiable lipids and monosaccharide carbohydrate contents are attributed to the characteristics of the *Chlorella* sp. ABC-001 under nitrogen-depleted conditions [29], which showed great potential for microalgal biorefinery feedstock.

**Table 1.** Biochemical composition of *Chlorella* sp. ABC-001. All the values are presented as the average of triplicated samples with standard deviations (n = 3).

Composition		Biomass (wt.%)	Crude Lipids <sup>2</sup> (wt.%)	Oil Phase (wt.%)	CASS Process <sup>3</sup>	
					Water Phase (wt.%)	Solid Phase <sup>4</sup> (wt.%)
Macromolecule composition <sup>1</sup>	Lipid	35.7 ± 0.6	35.7 ± 0.6	30.1 ± 0.2	N/A	2.2 ± 0.01
	Esterifiable Lipid (FAME)	29.8 ± 0.2	29.8 ± 0.2	27.0 ± 0.5		0.5 ± 0.2
	Carbohydrate	40.1 ± 1.3	N/A	N/A	29.1 ± 0.8	2.9 ± 0.1
	Glucose	19.1 ± 0.1			17.2 ± 0.3	0.2 ± 0.1
	Protein	18.7 ± 2.3	N/A	19.0 ± 0.4		
	Ash	5.5 ± 0.1	0.1 ± 0.1	<0.1	4.9 ± 0.0	0.5 ± 0.0
Elemental composition	C	51.8 ± 0.1	74.1 ± 0.6	75.4 ± 0.4	N/A	44.5 ± 0.1
	H	8.2 ± 0.1	11.8 ± 0.1	12.2 ± 0.1		6.5 ± 0.1
	O	29.7 ± 0.1	11.8 ± 0.1	11.4 ± 0.1		27.4 ± 0.0
	N	2.6 ± 0.0	0.4 ± 0.1	0.2 ± 0.0		8.2 ± 0.1
	S	0.2 ± 0.1	N/D	N/D		2.5 ± 0.1

<sup>1</sup> Macromolecule composition is based on the original dry biomass. <sup>2</sup> The composition of crude lipids extracted by the Folch Method will be discussed in Section 3.4. <sup>3</sup> The composition of the extraction mixture by the CASS process will be discussed in Section 3.4. <sup>4</sup> LEA (Lipid-extracted algae).

#### 3.2. Acid Pretreatment of Concentrated Wet Biomass

The effect of acid concentration, pretreatment time, and temperature was investigated using concentrated wet biomass (50 g/L) in terms of lipid extraction yield (Figure 2). To clarify the effects of acid treatment on the wet biomass, lipid recovery was performed using a conventional stirrer under overnight conditions to achieve mass transfer equilibrium. The lipid yield increased as the acid concentration, pretreatment time, and temperature increased and reached a saturation of around 90%. For acid concentration, only 0.5 wt.% sulfuric acid achieved 76% lipid yield and showed saturated behavior over 3 wt.% sulfuric acid, which is equivalent to 1.08 N concentration (Figure 2a). Lipid yield increased rapidly throughout the treatment and reached saturation point after 30 min (Figure 2b). Lipid yield was saturated at a temperature higher than 100 °C at 5 wt.% sulfuric acid condition (Figure 2c). The maximum lipid yield of 90.6% was achieved under the condition of 5 wt.%

sulfuric acid at 120 °C for 1 h. However, the difference compared to the second-highest temperature condition (100 °C) was insignificant, with a yield of 89.3%. Zhang et al. (2018) reported that they extracted 414.1 mg/g cell lipids with 0.5 M sulfuric acid at 120 °C for 1 h treatment from *Chlorella vulgaris* [38]. Martins et al. (2020) used 20 g/L of *Chlorella vulgaris* and achieved over 90% of lipid extraction yield with 5 vol.% sulfuric acids at 120 °C for 10 min treatment [39]. The results showed consistency with previous studies that concluded acid pretreatment requires more than 100 °C at diluted concentration.

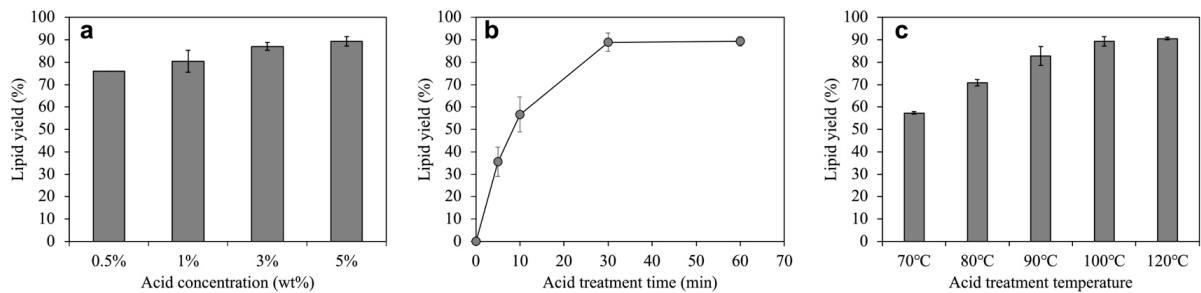


**Figure 2.** (a) Effect of acid concentration, (b) acid treatment time, and (c) acid treatment temperature on lipid extraction recovered by using a conventional stirrer at 1000 rpm for 12 h.

Providing enough thermal energy is key to inducing effective hydrolysis reactions. Cell morphology was observed through microscopic images after acid treatment at various temperature conditions (Figure 3). Before the acid treatment, the cell envelope exhibited a uniform circular shape with evenly distributed sizes of 3–5  $\mu\text{m}$  (Figure 3 (a)). As the temperature increased from 70 to 80 °C, cells began to agglomerate together without significant damage observed. Partial or complete destruction of cell walls was first found at 90 °C (Figure 3 (b)) and completely disrupted over 100 °C (Figure 3 (c)). At 120 °C, most cells were ruptured, resulting in the drainage of intracellular fluids from the cell envelope (Figure 3 (d)). The lipid droplets that remain in the intracellular fluids can easily be uptaken by organic solvents, even with low biomass concentration in a water medium. These results correspond with lipid yield results, showing that the destruction of cell walls is required to achieve a high lipid extraction yield of over 90%. Based on the above results, the acid treatment condition was fixed at 100 °C, 5 wt.% for 1 h on further research.

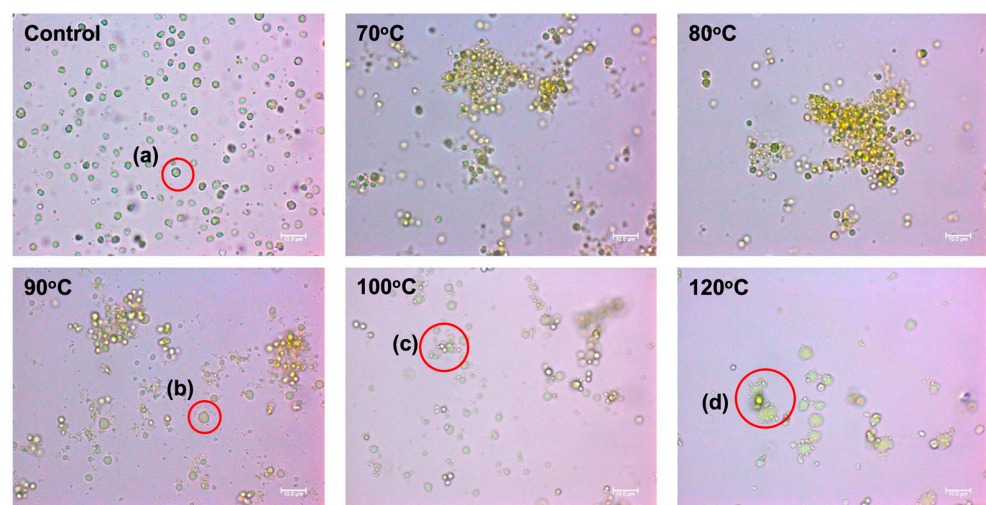


**Figure 3.** Microscopic image of *Chlorella* sp. ABC-001 before (control) and after acid treatment at various temperature conditions (5 wt.%, 1 h treatment). The scale bar is 10  $\mu\text{m}$ . Morphological changes are highlighted in red circles. (a) A normal cell; (b) the overall size of the cell is enlarged, and its shape starts to deviate from a sphere; (c) disrupted cells are agglomerated with cell debris; and (d) a complete cell rupture is observed.

### 3.3. Effects of Mixing Efficiency on the Lipid Recovery Process

The governing factor of the lipid recovery process is the mass transfer phenomenon, which can be defined as the mass transfer efficiency of lipid droplets into organic solvents through a water barrier [40]. The mass transfer rate is governed by diffusion, which is affected by surface area, concentration gradient between bulk solvent and biomass, and intrinsic diffusivity of lipids through the water layer. Even after the cell wall was ruptured by acid pretreatment, the polar water barrier hindered the extraction of lipids into solvents, reducing the recovery rate, which resulted in low process efficiency. Since our primary goal was to recover each of the biological components, especially the lipid, as much as possible economically, decreasing the time and increasing the yield were both important. Thus, a mechanical method of generating high-shear mixing was introduced to effectively deliver enough mixing energy to a water–organic solvent mixture.

Figure 4 shows the effects of the mixing efficiency of various rotational speeds of the HSM, and the conventional stirrer was compared in terms of lipid extraction yield and extraction time. The results demonstrated that increasing mixing speed affected lipid extraction yield and rate. In the case of the conventional stirrer, 500 and 750 rpm could not achieve a mass transfer saturation point due to their low mixing efficiency (Figure 4a). For 1000 rpm conditions, the saturation limit was achieved at about 85% after 6 h of treatment. On the other hand, the HSM exhibited higher lipid extraction efficiency than the stirrer at the same 1000 rpm, achieving the same level of extraction yield at 90 min, which matched the yield of the conventional stirrer at 180 min (Figure 4b). Even though the rotor diameter of the HSM and the stirrer was the same, the HSM's unique rotor–stator geometry generated additional shear force and turbulent flow, dramatically increasing mass transfer efficiency. As the rotational speed of the HSM increased, the saturation curve was achieved within 30 min at 3000 rpm and reached the highest yield of 90.7%.

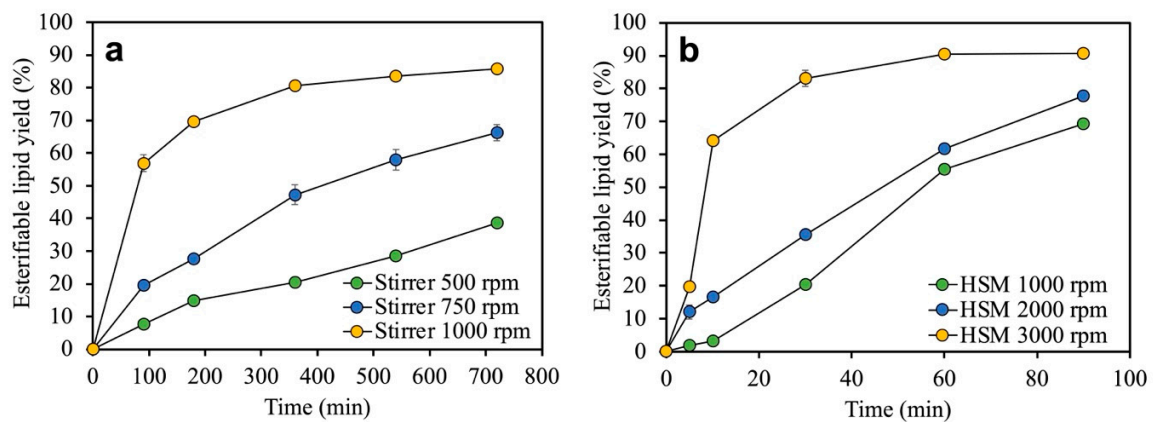


**Figure 4.** Effect of rotational speed and mixing time on the esterifiable lipid recovery yield using (a) a conventional stirrer and (b) a high-shear mixer after acid treatment (5 wt.%, 100 °C, 1 h).

The HSM was designed to be operated at high rpm conditions that could not be reached when using the conventional stirrer, and therefore, employing the HSM in the mixing process is beneficial in homogenizing immiscible fluids. The water and hexane need to contact the biomass as much as possible to recover responsible components for each phase. A number of papers provided proof-of-concept and optimization studies for high-shear-assisted solvent-based extraction in highly concentrated biomass conditions (>200 g dry cell/L) without water medium [12,41]. The extraction process with highly concentrated biomass could achieve a high yield with low solvent usage and energy consumption. However, the microalgae concentrating process requires extremely high energy and is time-consuming, necessitating proper selection and optimization of harvesting and extraction technology. Throughout the investigation presented in this study, the high-shear-assisted



extraction process has expanded its utility for recovering biological components from wet biomass at low concentrations.

### 3.4. Separation of Macromolecules in Post-Extracted Mixture: Biorefinery Concept

The previous section revealed that the CASS process can potentially extract lipids from low-concentration biomass with acid pretreatment and high-shear-assisted recovery. Since ABC-001 still contains significant sources of carbohydrates and proteins, it is necessary to clarify the extraction behavior of these macromolecules within the system to validate the potential of an algae-based biorefinery. Therefore, a comprehensive analysis of the mixtures in three phases (liquid–liquid–solid), consisting of water, an organic solvent containing lipids, and treated biomass, was performed from the perspective of macromolecules and other impurities, namely inorganic compounds. From the biomass, over 90% of the lipids and fermentable glucose were transferred into the organic solvent and water phases, respectively. All the protein contents were preserved (100%) in the lipid-extracted algae (LEA) layer (Figure 5). Notably, this phase separation was achieved naturally within 10 min after the CASS process. Details on each phase will be discussed in the following sub-chapters.

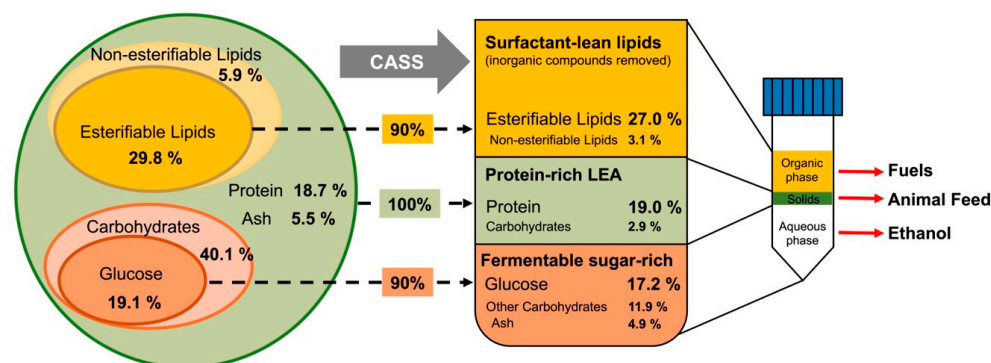


**Figure 5.** The composition and proposed use of three layers resulting from the natural separation of the extraction mixture obtained from the complete CASS process.

#### 3.4.1. Lipid Phase: Esterifiable Lipids Recovery

After the acid treatment and lipid recovery, the extracted mixture naturally separated into water, biomass residue, and hexane layers from bottom to top. The macromolecule analysis results are presented in Table 1, based on the weight percentage of the original biomass. The results indicated that lipids, carbohydrates, and proteins are distributed into oil, water, and solid phases, respectively. About 35.7 wt.% of lipids in the original biomass were distributed, with 30.1 wt.% in the oil phase and 2.2 wt.% in the lipid-extracted algae (LEA), respectively. In the case of fatty acid content, 27.0 wt.% was recovered by the oil phase, and only 0.5 wt.% remained in the solid phase, which is about 90% of the recovery yield from the original biomass.

Notably, the purity of the lipids extracted by the CASS process (89.7%) was higher than that of the conventional Folch method (83.5%). The lipids extracted by hexane usually have higher FAME contents than lipids extracted by the Folch method due to the higher polarity of chloroform/methanol than hexane, which could extract unwanted carbohydrates and protein-associated lipids [42]. Furthermore, acid treatment hydrolyzes galactolipids (MGDG, DGDG) and phospholipids (PE, PC), which are major components of chloroplasts and cell membranes, respectively, into polar functional groups and fatty acids [41].

Compared to the crude lipid extraction methods, the acid hydrolysis of polar lipids could cause a minor loss of total lipid contents in the CASS process. Total carbohydrate content increased slightly more than the original biomass, which indicates that the hydrolyzed galactose group was transferred into the water phase. The elemental analysis results further support the hydrolysis of unwanted polar lipids. In the oil phase, carbon and hydrogen

contents increased, and the oxygen and nitrogen contents decreased compared to the crude lipids. This observation is further supported by the hydrogen/carbon atomic ratio (H/C), an important descriptor that characterizes the quality of petroleum, which also can be applied in biomass-derived fuels in a slightly modified form, 'effective hydrogen-to-carbon ratio (H/C<sub>eff</sub>)', as defined as follows [43]:

$$H/C_{\text{eff}} = (n(\text{H}) - 2 \times n(\text{O}) - 3 \times n(\text{N}) - 2 \times n(\text{S}))/n(\text{C}) \quad (5)$$

where n(H), n(O), n(N), n(S), and n(C) represent the molar concentrations of hydrogen, oxygen, nitrogen, sulfur, and carbon, respectively. The H/C ratio of the oil phase from the CASS process was 1.71, whereas the crude lipids from the Folch method had a ratio of 1.66, implying that the quality of extracted lipids has been improved. When compared to the other type of extraction process, e.g., hydrothermal liquefaction (HTL), the CASS process achieved a higher value (1.71) than a previously reported study for the same species (1.56–1.63) [44], indicating that the lipid quality has been enhanced to be more suitable for fuels.

#### 3.4.2. Water Phase: Fermentable Glucose Recovery

The water phase contained 29.1 wt.% of total carbohydrates and 4.9 wt.% of inorganic compounds. The fermentable glucose was 17.2 wt.%, found in the water phase. This amount corresponds to 90% of the original biomass, and only 0.2 wt.% remained in the LEA. These results indicate that acid hydrolysis converted carbohydrates into fermentable glucose that is easily soluble in the water phase. The other carbohydrates remained in the algal cells, about 2.9 wt.% of the original biomass, corresponding to 7.2% of the original carbohydrate content. The final concentration of fermentable glucose in the water phase was 8.6 g/L. Meanwhile, the typical glucose concentration for yeast fermentation is more than 20 g/L [45]. This difference can be adjusted by concentrating the water phase or increasing biomass concentration. However, careful considerations should be taken when deciding on the adjustment since the capital costs may increase.

The other study using algal biomass first conducted lipid extraction, then carbohydrate hydrolysis, using lipid-extracted algae by applying post-acid treatments [46]. This concept has the advantage of uncoupling lipid extraction and carbohydrate hydrolysis, providing the flexibility to optimize each process independently, resulting in high yields of lipids and carbohydrates. On the other hand, the CASS process has the advantage of simultaneous lipid extraction and carbohydrate hydrolysis, achieving process simplification and requiring only two continuous mixing tanks and a three-phase separator, compared to the previous study that required more than two CSTRs and two separators for the continuous process [46]. Also, the earlier study applied a hexane/ethanol mixture (additional polar solvents) to achieve a high lipid yield, resulting in increased operating and raw material costs [39]. In the CASS process, high-shear mixing provided enough lipid extraction capabilities only with a non-polar solvent (hexane), without the assistance of polar solvents (e.g., methanol and ethanol).

#### 3.4.3. Solid Phase: Maintaining Protein Integrity

The solid phase is composed mainly of proteins, 56 wt.% of the LEA, corresponding to 18.8 wt.% of the original biomass. This indicates that most proteins remain in the biomass without being extracted. These results align with the elemental analysis results, given that LEA's nitrogen and sulfur content was 3.15 and 12.5 folds higher than the original biomass, respectively. Hydrolysis of protein into amino acids requires much harsher conditions than the CASS process, where the classical hydrolysis method used 6 N hydrochloric acid at 110 °C for 24 h treatment [47]. The original protein content appears preserved in LEA, making it suitable for nutritious animal and fish feeds [48].

### 3.4.4. Impurities Removal Effects on Extracted Lipids

The inorganic compounds, namely ashes, were mainly dissolved in water (90%), and the remaining amount was left in the LEA (10%). The detailed analysis of inorganic compounds (P, Ca, Na, K, Cu, Zn, Mg), performed using ICP analysis, is presented in Table 2. The results showed that most of the inorganic compounds were slipped into the water phase, the rest remained in the LEA, and only a small portion of phosphorus and copper were found in the oil phase. The phosphorus, mainly from phospholipids comprising cell membranes, was separated into water by acid hydrolysis. Phospholipids are the main impurities from bio-based feedstock that cause catalytic poisoning in the hydrodeoxygenation [49] and isomerization processes for biofuel production [50]. In the conventional process, phosphorus and other impurities are removed by a degumming process, which adds water and acid into crude lipids to separate impurities as a form of gum [51]. In the CASS process, acid treatment resulted in the pre-removal of impurities into the water phase, integrating lipid extraction and the degumming process.

**Table 2.** Inorganic compositions of *Chlorella* sp. ABC-001, crude lipids extracted by the Folch method, and products separated by the CASS process. All the values are presented as the average of triplicated samples with standard deviations (n = 3).

Content	Biomass (wt. ppm)	Crude Lipid <sup>1</sup> (wt. ppm)	Oil Phase (wt. ppm)	CASS Process Water Phase (wt. ppm)	Solid Phase <sup>2</sup> (wt. ppm)
P	27,021 ± 49	1130 ± 56	206.5 ± 1.9	24,318 ± 155	3346 ± 155
Ca	3168 ± 69	74.5 ± 5.1	N/D	2738 ± 21	461.2 ± 5.3
Na	623 ± 5	N/D	N/D	792.8 ± 6.7	137.4 ± 3.3
K	19,844 ± 509	65.3 ± 1.8	N/D	17,344 ± 242	312.9 ± 2.0
Cu	889 ± 37	271.8 ± 8.2	24.9 ± 1.3	700.7 ± 0.4	352.1 ± 5.1
Zn	232 ± 53	17.4 ± 1.8	N/D	298.1 ± 0.7	N/D
Mg	3325 ± 44	N/D	N/D	2891 ± 5	574.0 ± 10.2

<sup>1</sup> The composition of crude lipids extracted by the Folch method. <sup>2</sup> LEA.

The CASS process induced a stable phase separation without forming an emulsion. Emulsion formation, a critical issue in the two-step cell disruption and lipid extraction process, causes a loss of lipids and carbohydrates by trapping them within the emulsion layer and significantly increases the costs of additional separation [52]. High biomass concentrations and the severity of cell disruption increase the chance of emulsion formation due to the secretion of bio-surfactants, which mainly consist of phospholipids, small carbohydrates, and proteins [53]. In fact, ABC-001 also formed an emulsion when concentrated biomass was directly mixed with hexane using a high-shear mixer without acid pretreatment, indicating the presence of bio-surfactants. As demonstrated in this study, hydrolysis of phospholipids and carbohydrates prevented emulsion formation, obtaining a clear phase separation after vigorous high-shear mixing. Applying acid pretreatment at the low biomass concentration was beneficial not only for the proper distribution of macromolecules, but also for preventing emulsion formation during lipid recovery.

### 3.5. Comparison with Other Biorefinery Processes

Many researchers have reported several methods to fractionate macromolecules (Table 3). Most of them used a combination of acid hydrolysis (pretreatment) and solvent extraction, similar to our approach, focusing on the simultaneous production of biofuel and bioethanol. Nonetheless, there is a significant difference between CASS and the other studies. This study presents all the components' conversion ratios in different phases, discussing the quality of products to take practical issues such as emulsification and catalytic poisoning into account.

Table 3. Comparison of the microalgal biorefinery processes.

Process	Strains	Biomass Conc. (g/L)	Operating Conditions	Macromolecule Yield (%)	References
High-pressure homogenizer	<i>Nannochloropsis</i> sp.	110–230	(1) Cell weakening (35 °C, 7–24 h) (2) High-pressure homogenizer (800–1000 bar, 1 pass) (3) Lipid recovery (2 h, biomass (paste):solvent 5:2 w/w)	Lipid: 25 Carbohydrate in water: 41 Protein in biomass: 51	[54]
Acid hydrolysis	<i>Tribonema</i> sp.	50	(1) Acid hydrolysis (3 wt%, sulfuric acid, 121 °C, 45 min) (2) Lipid recovery (ethanol-hexane (1:3, v/v) on shaker incubation, 2.5 h, 50 °C, biomass (paste):solvent = 1:6 v/v)	Biodiesel: 98.5 Monosaccharides: 81.5	[55]
Acid hydrolysis	<i>Chlorella</i> sp. <i>Scenedesmus</i> sp.	250	(1) Acid hydrolysis (2 wt%, sulfuric acid, 155 °C, 10 min) (2) Lipid recovery (hexane, 2 h, biomass (paste):solvent 1:1 v/v)	Lipid: 22.2 Glucose: 81.2 Lipid: 92.5 Glucose: 73.1	[56]
Acid hydrolysis	<i>Chlorella</i> sp. ABC-001	50	(1) Acid hydrolysis (0.1 N, sulfuric acid, 170 °C, 4 min) (2) Phase separation using centrifugation (1000 rpm, 5 min) (3) Lipid recovery (hexane with vortexing, 20 min)	Lipid: 100 Monosaccharides: 89	[57]
Hydrothermal liquefaction	<i>Chlorella</i> sp. KR1	50	(1) Hydrothermal liquefaction (180 °C, 1 h) (2) Lipid recovery (hexane with sonication, 2 h)	Lipid: 87 Glucose: 70	[49]
CASS	<i>Chlorella</i> sp. ABC-001	50	(1) Acid hydrolysis (5 wt.% sulfuric acid, 100 °C, 1 h) (2) Lipid recovery (hexane with high-shear mixing, 3000 rpm, 30 min, biomass (wet):solvent = 1:1 v/v)	Lipid: 90.6 Glucose: 90.0 Protein: 100	This study

Halim et al. (2016) employed a high-pressure homogenizer to disrupt the strong cell wall of *Nannochloropsis* sp. and monitored the yield of the macromolecules' recovery, which included 25% of lipids, 41% of carbohydrates, and 51% of proteins [54]. Although a comprehensive biorefinery concept was proposed and analyzed, most macromolecule components, especially lipids, were trapped in the emulsion layer. Since protein plays a significant role in emulsion formation, species enriched in carbohydrates and lipids while lacking in protein have been favored for the complete fractionation and utilization of macromolecules. Wang et al. (2014) used *Tribonema* sp., which has very low protein contents, for biodiesel and monosaccharide production [55]. Laurence et al. (2015) used *Chlorella* sp., which is also low in protein, but obtained low lipid recovery since they employed the conventional stirrer for the extraction [56].

In the same context, *Chlorella* sp. ABC-001, which accumulates high levels of lipids and carbohydrates, has been studied for biorefinery applications. Seon et al. (2023) adopted acid hydrolysis under lower acidic concentration (0.1 N) at higher temperatures (170 °C) than this study, followed by centrifugation of hydrolysate for volume reduction, and then solvent extraction [57]. The yields were high (lipids of 100% and monosaccharides of 89%), but this process required additional steps for phase separation and holds a potential concern for corrosion issues due to high temperatures. Jin et al. (2017) used hydrothermal liquefaction (HTL) instead of acid hydrolysis and then recovered lipids using solvents from *Chlorella* sp. KR1 [49], which had a similar compositional character to ABC-001. The lipid yield was comparable to this study (87%), but conversion of carbohydrates (70%) was low for bioethanol fermentation.

The novelties of the CASS process and this study are (1) the application of a high-shear mixer to disrupt the water barrier in mildly concentrated wet biomass, (2) a comprehensive analysis of macromolecule conversion, and (3) the demonstration of acid hydrolysis's effects on both carbohydrate saccharification and phospholipid breakdown. The use of high-shear mixing enabled the efficient processing of low-concentration wet biomass at a relatively low biomass-to-solvent ratio (1:1 v/v), resulting in a high lipid yield exceeding 90%. The effects of acid pretreatment were thoroughly investigated, with the expanded scope of analysis encompassing overall macromolecule yield and quality. Carbohydrate hydrolysis

produced a glucose yield of 90%, surpassing other studies. Additionally, phospholipid hydrolysis transferred hydrophilic polar heads to the aqueous phase, thereby preventing emulsion formation in the solvent phase and minimizing product loss. As discussed in the previous paragraph, emulsion formation is a significant operational challenge that has been extensively recognized. This issue was effectively mitigated by applying hydrolysis prior to high-shear mixing. Notably, protein remains undegraded under mild acidic conditions, allowing it to be preserved in the solid phase (LEA) for potential use in nutritional feeds. Moreover, the removal of inorganic compounds from the lipids reduces the risk of catalytic poisoning in the following processes. The CASS process is well suited for providing high yields while maintaining product integrity as a bridging extraction process between harvesting/dewatering and catalytic conversion in the whole biorefinery concept. Furthermore, the CASS process is scalable, as high-shear mixers are commercially available for large-scale production and have proven effective [28]. As the diameter of the rotor increases, so does the Reynolds number, enhancing turbulent mixing efficiency relative to energy consumption [12].

#### 4. Conclusions

The CASS process was developed by combining acid pretreatment and high-shear-assisted extraction to efficiently separate macromolecules from microalgae biomass. Acid treatment effectively hydrolyzed phospholipids (biosurfactants) and removed inorganic compounds (potential catalytic poisons), enabling the recovery of more than 90% of esterifiable lipids with improved quality in the following high-shear-assisted extraction using hexane. Simultaneously, over 90% of the glucose was hydrolyzed into the water phase at a concentration of 8.7 g/L, making it suitable for bioethanol fermentation. Due to the mild acid concentration, proteins were preserved in the solid lipid-extracted algae phase without any loss (100%). The extraction mixture did not suffer from emulsification but formed stable layers of solvent, water, and solids, each rich in lipids, glucose, and protein, without requiring additional separation processes. The CASS process shows potential for scalable biorefineries to fractionate nutrient-replete ABC-001 biomass for the co-production of biofuel, bioethanol, and nutritious animal feed. Future research could investigate the applicability of this process to other microalgal species, conduct techno-economic analysis for different target products under various cultivation scenarios, and include sensitivity analysis to assess the impact of biomass composition on economic feasibility.

**Author Contributions:** D.K.—Conceptualization, data curation, writing—original draft, writing—review and editing, funding acquisition; S.-G.K.—conceptualization, formal analysis, methodology, writing—original draft; Y.K.C.—project administration, resources, supervision; M.K.—conceptualization, data curation, writing—original draft, writing—review and editing, visualization, supervision. All authors have read and agreed to the published version of the manuscript.

**Funding:** This work was supported by Qatar University QUT2RP-CENG-24/25-501. The findings achieved herein are solely the responsibility of the authors.

**Institutional Review Board Statement:** Not applicable.

**Informed Consent Statement:** Not applicable.

**Data Availability Statement:** Data are contained within the article.

**Conflicts of Interest:** The authors declare no conflicts of interest.

#### References

1. Spandagos, C. Achieving decarbonization goals through biofuels: Policy challenges and opportunities in the European Union and the United States. In *Advances in Biofuels Production, Optimization and Applications*; Elsevier: Amsterdam, The Netherlands, 2024; pp. 269–283.
2. Bracmort, K. *The Renewable Fuel Standard (RFS): An Overview*; Congressional Research Service: Washington, DC, USA, 2023.
3. Bhatt, A.H.; Zhang, Y.; Milbrandt, A.; Newes, E.; Moriarty, K.; Klein, B.; Tao, L. Evaluation of performance variables to accelerate the deployment of sustainable aviation fuels at a regional scale. *Energy Convers. Manag.* **2023**, *275*, 116441. [[CrossRef](#)]



4. Halim, R.; Danquah, M.K.; Webley, P.A. Extraction of oil from microalgae for biodiesel production: A review. *Biotechnol. Adv.* **2012**, *30*, 709–732. [[CrossRef](#)] [[PubMed](#)]
5. Chisti, Y. Biodiesel from microalgae. *Biotechnol. Adv.* **2007**, *25*, 294–306. [[CrossRef](#)] [[PubMed](#)]
6. Wijffels, R.H.; Barbosa, M.J. An Outlook on Microalgal Biofuels. *Science* **2010**, *329*, 796–799. [[CrossRef](#)]
7. Klein, B.C.; Chagas, M.F.; Davis, R.E.; Watanabe, M.D.; Wiatrowski, M.R.; Morais, E.R.; Laurens, L.M. A systematic multicriteria-based approach to support product portfolio selection in microalgae biorefineries. *Chem. Eng. J.* **2024**, *481*, 148462. [[CrossRef](#)]
8. Kruger, J.S.; Wiatrowski, M.; Davis, R.E.; Dong, T.; Knoshaug, E.P.; Nagle, N.J.; Laurens, L.M.; Pienkos, P.T. Enabling production of algal biofuels by techno-economic optimization of co-product suites. *Front. Chem. Eng.* **2022**, *3*, 803513. [[CrossRef](#)]
9. Olguín, E.J.; Sánchez-Galván, G.; Arias-Olguín, I.I.; Melo, F.J.; González-Portela, R.E.; Cruz, L.; De Philippis, R.; Adessi, A. Microalgae-based biorefineries: Challenges and future trends to produce carbohydrate enriched biomass, high-added value products and bioactive compounds. *Biology* **2022**, *11*, 1146. [[CrossRef](#)]
10. Andreeva, A.; Budenkova, E.; Babich, O.; Sukhikh, S.; Dolganyuk, V.; Michaud, P.; Ivanova, S. Influence of carbohydrate additives on the growth rate of microalgae biomass with an increased carbohydrate content. *Mar. Drugs* **2021**, *19*, 381. [[CrossRef](#)]
11. Sed, G.; Cicci, A.; Jessop, P.G.; Bravi, M. A novel switchable-hydrophilicity, natural deep eutectic solvent (NaDES)-based system for bio-safe biorefinery. *RSC Adv.* **2018**, *8*, 37092–37097. [[CrossRef](#)]
12. Kwak, M.; Roh, S.; Yang, A.; Lee, H.; Chang, Y.K. High shear-assisted solvent extraction of lipid from wet biomass of *Aurantiochytrium* sp. KRS101. *Sep. Purif. Technol.* **2019**, *227*, 115666. [[CrossRef](#)]
13. Ramasubramania, I. The issue of reducing or removing phospholipids from total lipids of a microalgae and an oleaginous fungus for preparing biodiesel. *Biofuels* **2016**, *7*, 55–72.
14. Arora, P. Deactivation of Catalysts and Reaction Kinetics for Upgrading of Renewable Oils. Ph.D. Thesis, Chalmers Tekniska Hogskola, Gothenburg, Sweden, 2019.
15. Nitsos, C.; Filali, R.; Taidi, B.; Lemaire, J. Current and novel approaches to downstream processing of microalgae: A review. *Biotechnol. Adv.* **2020**, *45*, 107650. [[CrossRef](#)]
16. Avelo, M.I.; Horrocks, L.A. Quantitative release of fatty acids from lipids by a simple hydrolysis procedure. *J. Lipid Res.* **1983**, *24*, 1101–1105. [[CrossRef](#)] [[PubMed](#)]
17. Rinaldi, R.; Schüth, F. Acid hydrolysis of cellulose as the entry point into biorefinery schemes. *ChemSusChem Chem. Sustain. Energy Mater.* **2009**, *2*, 1096–1107. [[CrossRef](#)]
18. Wijaya, Y.P.; Putra, R.D.D.; Widyaya, V.T.; Ha, J.-M.; Suh, D.J.; Kim, C.S. Comparative study on two-step concentrated acid hydrolysis for the extraction of sugars from lignocellulosic biomass. *Bioresour. Technol.* **2014**, *164*, 221–231. [[CrossRef](#)] [[PubMed](#)]
19. Sukias, J.; Craggs, R. Enhanced methane yields from microalgal digestion with various pre-treatments. In Proceedings of the 7th IWA Specialist Group Conference on Waste Stabilization Ponds, Bangkok, Thailand, 25–27 September 2006; pp. 25–27.
20. Sposob, M.; Kim, D.-H.; Yun, G.-S.; Yun, Y.-M. Assessment of the relationship between solubilization and biogas production on anaerobic digestion of pretreated lipid-extracted microalgae waste. *Biomass Bioenergy* **2020**, *141*, 105702. [[CrossRef](#)]
21. Santos, N.O.; Oliveira, S.M.; Alves, L.C.; Cammarota, M.C. Methane production from marine microalgae *Isochrysis galbana*. *Bioresour. Technol.* **2014**, *157*, 60–67. [[CrossRef](#)]
22. Samson, R.; Leduy, A. Influence of mechanical and thermochemical pretreatments on anaerobic digestion of *Spirulina maxima* algal biomass. *Biotechnol. Lett.* **1983**, *5*, 671–676. [[CrossRef](#)]
23. Rincón-Pérez, J.; Razo-Flores, E.; Morales, M.; Alatríste-Mondragón, F.; Celis, L.B. Improving the biodegradability of *Scenedesmus obtusiusculus* by thermochemical pretreatment to produce hydrogen and methane. *BioEnergy Res.* **2020**, *13*, 477–486. [[CrossRef](#)]
24. Marques, A.d.L.; Pinto, F.P.; Araújo, O.Q.d.F.; Cammarota, M.C. Assessment of methods to pretreat microalgal biomass for enhanced biogas production. *J. Sustain. Dev. Energy Water Environ. Syst.* **2018**, *6*, 394–404. [[CrossRef](#)]
25. Juárez, J.M.; Pastor, E.R.; Sevilla, J.M.F.; Torre, R.M.; García-Encina, P.A.; Rodríguez, S.B. Effect of pretreatments on biogas production from microalgae biomass grown in pig manure treatment plants. *Bioresour. Technol.* **2018**, *257*, 30–38. [[CrossRef](#)] [[PubMed](#)]
26. Cheng, Q.; Deng, F.; Li, H.; Qin, Z.; Wang, M.; Li, J. Nutrients removal from the secondary effluents of municipal domestic wastewater by *Oscillatoria tenuis* and subsequent co-digestion with pig manure. *Environ. Technol.* **2018**, *39*, 3127–3134. [[CrossRef](#)] [[PubMed](#)]
27. Phwan, C.K.; Chew, K.W.; Sebayang, A.H.; Ong, H.C.; Ling, T.C.; Malek, M.A.; Ho, Y.-C.; Show, P.L. Effects of acids pre-treatment on the microbial fermentation process for bioethanol production from microalgae. *Biotechnol. Biofuels* **2019**, *12*, 191. [[CrossRef](#)]
28. Zhang, J.; Xu, S.; Li, W. High shear mixers: A review of typical applications and studies on power draw, flow pattern, energy dissipation and transfer properties. *Chem. Eng. Process. Process Intensif.* **2012**, *57–58*, 25–41. [[CrossRef](#)]
29. Cho, J.M.; Oh, Y.K.; Park, W.K.; Chang, Y.K. Effects of Nitrogen Supplementation Status on CO<sub>2</sub> Biofixation and Biofuel Production of the Promising Microalga *Chlorella* sp. ABC-001. *J. Microbiol. Biotechnol.* **2020**, *30*, 1235–1243. [[CrossRef](#)]
30. Bilad, M.; Arafat, H.A.; Vankelecom, I.F. Membrane technology in microalgae cultivation and harvesting: A review. *Biotechnol. Adv.* **2014**, *32*, 1283–1300. [[CrossRef](#)]
31. Kim, D.; Kwak, M.; Kim, K.; Chang, Y.K. Turbulent jet-assisted microfiltration for energy efficient harvesting of microalgae. *J. Membr. Sci.* **2019**, *575*, 170–178. [[CrossRef](#)]
32. Folch, J.; Lees, M.; Sloane Stanley, G.H. A simple method for the isolation and purification of total lipides from animal tissues. *J. Biol. Chem.* **1957**, *226*, 497–509. [[CrossRef](#)]

33. Kwak, M.; Kang, S.G.; Hong, W.-K.; Han, J.-I.; Chang, Y.K. Simultaneous cell disruption and lipid extraction of wet *Aurantiocytrium* sp. KRS101 using a high shear mixer. *Bioprocess Biosyst. Eng.* **2018**, *41*, 671–678. [[CrossRef](#)]
34. DuBois, M.; Gilles, K.A.; Hamilton, J.K.; Rebers, P.A.; Smith, F. Colorimetric Method for Determination of Sugars and Related Substances. *Anal. Chem.* **1956**, *28*, 350–356. [[CrossRef](#)]
35. Seon, G.; Joo, H.W.; Kim, Y.J.; Park, J.; Chang, Y.K. Hydrolysis of lipid-extracted *Chlorella vulgaris* by simultaneous use of solid and liquid acids. *Biotechnol. Prog.* **2019**, *35*, e2729. [[CrossRef](#)]
36. Laurens, L.M.L.; Dempster, T.A.; Jones, H.D.T.; Wolfrum, E.J.; Van Wychen, S.; McAllister, J.S.P.; Rencenberger, M.; Parcher, K.J.; Gloe, L.M. Algal Biomass Constituent Analysis: Method Uncertainties and Investigation of the Underlying Measuring Chemistries. *Anal. Chem.* **2012**, *84*, 1879–1887. [[CrossRef](#)]
37. Cho, E.J.; Trinh, L.T.P.; Song, Y.; Lee, Y.G.; Bae, H.-J. Bioconversion of biomass waste into high value chemicals. *Bioresour. Technol.* **2020**, *298*, 122386. [[CrossRef](#)]
38. Zhang, C.; Tang, X.; Yang, X. Overcoming the cell wall recalcitrance of heterotrophic *Chlorella* to promote the efficiency of lipid extraction. *J. Clean. Prod.* **2018**, *198*, 1224–1231. [[CrossRef](#)]
39. Martins, L.B.; Soares, J.; da Silveira, W.B.; Sousa, R.d.C.S.; Martins, M.A. Dilute sulfuric acid hydrolysis of *Chlorella vulgaris* biomass improves the multistage liquid-liquid extraction of lipids. *Biomass Convers. Biorefinery* **2021**, *11*, 2485–2497. [[CrossRef](#)]
40. Ranjan, A.; Patil, C.; Moholkar, V.S. Mechanistic assessment of microalgal lipid extraction. *Ind. Eng. Chem. Res.* **2010**, *49*, 2979–2985. [[CrossRef](#)]
41. Kwak, M.; Kim, D.; Kim, S.; Lee, H.; Chang, Y.K. Solvent screening and process optimization for high shear-assisted lipid extraction from wet cake of *Nannochloropsis* sp. *Renew. Energy* **2020**, *149*, 1395–1405. [[CrossRef](#)]
42. Gong, M.; Hu, Y.; Yedahalli, S.; Bassi, A. Oil extraction processes in microalgae. *Recent Adv. Renew. Energy* **2017**, *1*, 377–411.
43. Huber, G.W.; Corma, A. Synergies between bio- and oil refineries for the production of fuels from biomass. *Angew. Chem. Int. Ed.* **2007**, *46*, 7184–7201. [[CrossRef](#)] [[PubMed](#)]
44. Jin, M.; Oh, Y.-K.; Chang, Y.K.; Choi, M. Optimum utilization of biochemical components in *Chlorella* sp. KR1 via subcritical hydrothermal liquefaction. *ACS Sustain. Chem. Eng.* **2017**, *5*, 7240–7248. [[CrossRef](#)]
45. Zhang, Q.; Wu, D.; Lin, Y.; Wang, X.; Kong, H.; Tanaka, S. Substrate and Product Inhibition on Yeast Performance in Ethanol Fermentation. *Energy Fuel* **2015**, *29*, 1019–1027. [[CrossRef](#)]
46. Yun, J.-H.; Nam, J.-W.; Yang, J.H.; Lee, Y.J.; Cho, D.-H.; Choi, H.I.; Hong, J.S.; Ahn, K.H.; Kim, H.-S. Toward a zero-waste microalgal biorefinery: Complete utilization of defatted *Chlorella* biomass as a sole heterotrophic substrate for *Chlorella* sp. HS2 and an improved composite filler. *Chem. Eng. J.* **2024**, *480*, 147998. [[CrossRef](#)]
47. Gehrke, C.W.; Wall Sr, L.L.; Absheer, J.S.; Kaiser, F.E.; Zumwalt, R.W. Sample preparation for chromatography of amino acids: Acid hydrolysis of proteins. *J. Assoc. Off. Anal. Chem.* **1985**, *68*, 811–821. [[CrossRef](#)]
48. Singh, A.K.; Prajapati, K.S.; Shuaib, M.; Kushwaha, P.P.; Kumar, S. Microbial proteins: A potential source of protein. In *Functional Foods and Nutraceuticals: Bioactive Components, Formulations and Innovations*; Springer: Cham, Switzerland, 2020; pp. 139–147.
49. Abdus Salam, M.; Creaser, D.; Arora, P.; Tamm, S.; Lind Grennfelt, E.; Olsson, L. Influence of bio-oil phospholipid on the hydrodeoxygenation activity of NiMoS/Al<sub>2</sub>O<sub>3</sub> catalyst. *Catalysts* **2018**, *8*, 418. [[CrossRef](#)]
50. van der Bij, H.E.; Weckhuysen, B.M. Phosphorus promotion and poisoning in zeolite-based materials: Synthesis, characterisation and catalysis. *Chem. Soc. Rev.* **2015**, *44*, 7406–7428. [[CrossRef](#)]
51. Paisan, S.; Chetpattananondh, P.; Chongkhong, S. Assessment of water degumming and acid degumming of mixed algal oil. *J. Environ. Chem. Eng.* **2017**, *5*, 5115–5123. [[CrossRef](#)]
52. Law, S.Q.; Chen, B.; Scales, P.J.; Martin, G.J. Centrifugal recovery of solvent after biphasic wet extraction of lipids from a concentrated slurry of *Nannochloropsis* sp. biomass. *Algal Res.* **2017**, *24*, 299–308. [[CrossRef](#)]
53. Law, S.Q.; Mettu, S.; Ashokkumar, M.; Scales, P.J.; Martin, G.J. Emulsifying properties of ruptured microalgae cells: Barriers to lipid extraction or promising biosurfactants? *Colloids Surf. B Biointerfaces* **2018**, *170*, 438–446. [[CrossRef](#)] [[PubMed](#)]
54. Halim, R.; Webley, P.A.; Martin, G.J. The CIDES process: Fractionation of concentrated microalgal paste for co-production of biofuel, nutraceuticals, and high-grade protein feed. *Algal Res.* **2016**, *19*, 299–306. [[CrossRef](#)]
55. Wang, H.; Ji, C.; Bi, S.; Zhou, P.; Chen, L.; Liu, T. Joint production of biodiesel and bioethanol from filamentous oleaginous microalgae *Tribonema* sp. *Bioresour. Technol.* **2014**, *172*, 169–173. [[CrossRef](#)]
56. Laurens, L.; Nagle, N.; Davis, R.; Sweeney, N.; Van Wychen, S.; Lowell, A.; Pienkos, P. Acid-catalyzed algal biomass pretreatment for integrated lipid and carbohydrate-based biofuels production. *Green Chem.* **2015**, *17*, 1145–1158. [[CrossRef](#)]
57. Seon, G.; Kim, M.; Lee, Y.W.; Cho, J.M.; Kim, H.; Park, W.-K.; Chang, Y.K. Development of an integrated biomass refinery process for whole cell biomass utilization of *Chlorella* sp. ABC-001. *Chem. Eng. J.* **2023**, *451*, 138543. [[CrossRef](#)]

**Disclaimer/Publisher's Note:** The statements, opinions and data contained in all publications are solely those of the individual author(s) and contributor(s) and not of MDPI and/or the editor(s). MDPI and/or the editor(s) disclaim responsibility for any injury to people or property resulting from any ideas, methods, instructions or products referred to in the content.